

Topological Semantic Mapping by Consolidation of Deep Visual Features

Ygor C. N. Sousa¹ and Hansenclever F. Bassani¹

Abstract—Many works in the recent literature introduce semantic mapping methods that use CNNs (Convolutional Neural Networks) to recognize semantic properties in images. The types of properties (eg.: room size, place category, and objects) and their classes (eg.: kitchen and bathroom, for place category) are usually predefined and restricted to a specific task. Thus, all the visual data acquired and processed during the construction of the maps are lost and only the recognized semantic properties remain on the maps. In contrast, this work introduces a topological semantic mapping method that uses deep visual features extracted by a CNN, the GoogLeNet, from 2D images captured in multiple views of the environment as the robot operates, to create consolidated representations of visual features acquired in the regions covered by each topological node. These consolidated representations allow flexible recognition of semantic properties of the regions and use in a range of visual tasks. The experiments, performed using a real-world indoor dataset, showed that the method is able to consolidate the visual features of regions and use them to recognize objects and place categories as semantic properties, and to indicate the topological location of images, with very promising results. The objects are classified using the classification layer of GoogLeNet, without retraining, and the place categories are recognized using a shallow Multilayer Perceptron.

I. INTRODUCTION

The semantic mapping process involves using machine learning methods to infer semantic properties (eg.: room size, place category, and objects) of the mapped environments at a metric or topological level [1], [2]. Many methods proposed in recent works use CNNs (Convolutional Neural Networks) to recognize semantic properties through classification, object detection and semantic segmentation in images and integrate the results with metric or topological maps in several different approaches [3], [4], [5], [6], [7], [8], [9], [10], [11], [12], [13], [14], [15], [16].

Despite the benefits of using CNNs, training this type of neural network is costly in terms of time and resources. Using pre-trained CNNs is an alternative already present in the recent semantic mapping literature. Some works use a pre-trained CNN and perform transfer learning, fine-tuning it to recognize task-specific semantic information in the images [3], [4], [8], [16]. Others use a pre-trained CNN to perform the recognition of semantic properties without any changes or retraining [6], [14], [9], [12], [13], [15].

Most semantic mapping methods attach to the maps single-view semantic information recognized from images with se-

This work was supported by the Brazilian Coordination for Improvement of Higher Education Personnel (CAPES).

¹The authors are with the Centro de Informática, Universidade Federal de Pernambuco, Recife, PE, 50.740-560, Brazil {ycns, hfb}@cin.ufpe.br

mantic data accumulated or fused over time [4], [5], [6], [10], [11], [12], [14]. Other methods change the common approach of working only in single-view and acquire semantic information by performing multi-view semantic segmentation [7], [8]. However, the types of semantic properties recognized are usually previously defined and thus restricted to what was expected. Due to these restrictions, the large amount of the visual data acquired and processed by the agent during the building process of the maps is lost, no new semantic recognition can be made from them, and only the recognized semantic properties remain on the maps.

In this context, the present work introduces a topological semantic mapping method that uses deep visual features extracted from 2D images acquired in multiple perspectives of the environment as the agent operates, to create consolidated representations of visual features acquired in the regions covered by each topological node. The consolidated representations allow flexible recognition of semantic properties of the regions and use in other types of visual tasks. The method uses a pre-trained CNN, the GoogLeNet (Inception v1) [17], to extract the features from the images captured by the robotic agent. The features are extracted from a deep latent layer of the CNN and consolidated into the nodes of a topological map, in a process inspired by Self-Organizing Maps (SOM) [18]. In this work, the consolidated representations are used to perform the classification of objects and place categories as semantic properties of the regions covered by the nodes. The objects are classified using the classification layer of GoogLeNet, without retraining, and the place categories are recognized using an MLP (Multilayer Perceptron) with a single hidden layer.

The method was evaluated in experiments using the COLD dataset (COsy Localization Database) [19], a real-world indoor dataset, with which the method was able to build proper maps and consolidate visual features used to recognize semantic properties (objects and place categories) of regions with very promising results. This work also introduces an approach to locate images on the maps as a demonstration of application of the consolidated representations in a different visual task. The image localization approach was used in the experiments and the results suggested that the consolidated representations did not degrade as more data was provided and were representative enough to be used in the task.

II. RELATED WORK

Many works in the literature of semantic mapping use CNNs to recognize semantic properties in various types of approaches and applications. In [4], McCormac et al.

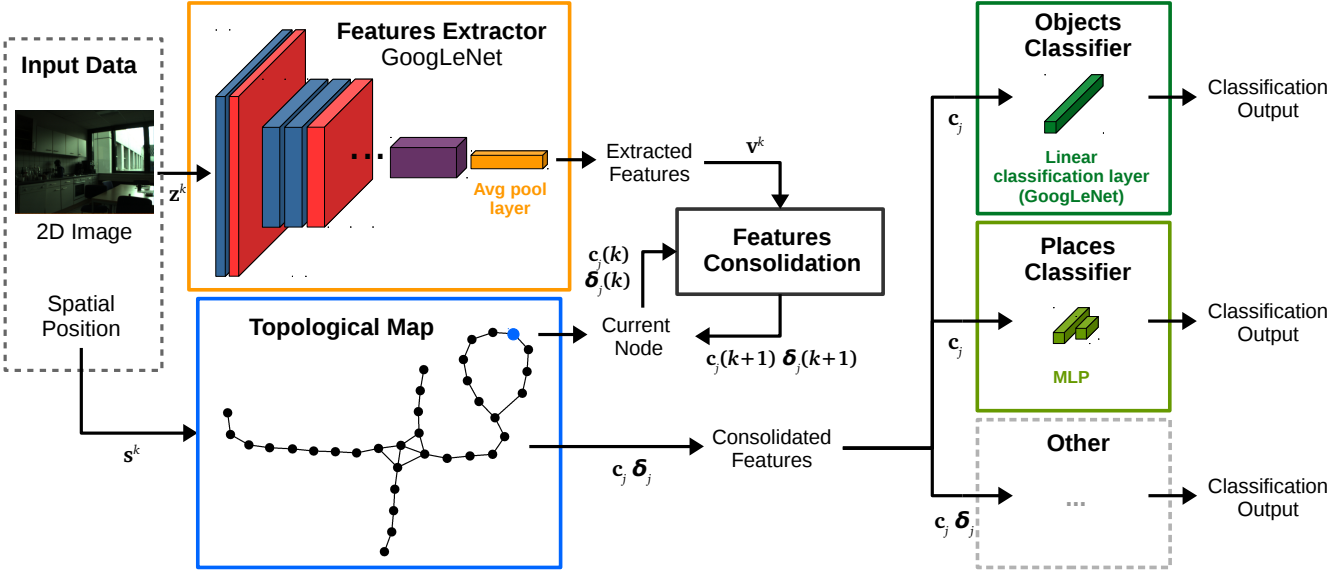


Fig. 1. Overview of the method: the GoogLeNet extracts the visual features of the input images and the nodes on the topological map corresponding to the input positions consolidate the extracted features in their representations; The consolidated features in each node are provided to the classification layer of the GoogLeNet (without retraining) and the objects visualized by the agent in the nodes are obtained; The consolidated features in each node are also provided to a shallow MLP and the place category of each node is obtained; Other semantic properties could be recognized from the consolidated features, but this work is limited to the objects and place categories.

use a CNN to perform semantic segmentation of images and incorporate the predictions into a dense 3D metric map. In a method created for Micro-Aerial Vehicles (MAV), Maturana et al. [5] present a CNN designed for fast on-board processing. The CNN performs semantic segmentation of images and the 2D measurements are aggregated into a 2.5D grid map. In other work, Maturana et al. [10] propose a CNN designed to perform semantic segmentation and incorporate the semantic information into a 2.5D grid map for off-road autonomous driving. Bernuy and Ruiz-del-Solar [11] use a CNN to perform semantic segmentation of images and the output labels are accumulated in histograms that are used to assist the creation of topological maps.

In a hybrid metric-topological semantic mapping approach, Lou and Chiou [12] use a CNN to detect objects in a mapping system with multiple levels of semantic information. In [6], Sunderhauf et al. detect objects in images using a pre-trained CNN and integrate the results into a 3D sparse metric map, where a 3D unsupervised segmentation method is used to assign segments of 3D points of the map to the detected objects. Nakajima and Saito [13] use a pre-trained CNN to detect objects in images and improve 3D maps with object-oriented semantic information in an efficient framework.

The method introduced by Xiang and Fox [8] presents a recurrent approach that accumulates features extracted with a CNN to perform multi-view semantic segmentation in a joint 3D scene semantic mapping process. Despite the advances in the method that allow the accumulation of features from multiple views, the method does not create representations of regions that can be used to obtain other semantic information and the accumulated features are used only to label pixels

of images.

Some works use pre-trained CNNs integrated with other machine learning approaches to allow incremental learning of new classes of a semantic property. In [3], Sunderhauf et al. introduce a model that learns incrementally new categories of places, in a supervised fashion, by extending a CNN with an one-vs-all Random Forest classifier. Rangel et al. [14] present a semantic mapping method that exploits CNNs previously trained to classify unlabeled images and perform a bottom-up aggregation approach that clusters images in the same semantic category. In [9], Sousa and Bassani presented a topological semantic mapping approach that incrementally and in an on-line fashion, forms clusters of object vectors classified with a pre-trained CNN. The clusters are formed using a SOM-based method and represent the categories of visited places. However, even with the efforts to allow semantic mapping methods to incorporate new semantic classes incrementally, these methods are still restricted to previously defined types of semantic properties.

In contrast, the present work introduces a method that creates consolidated representations of visual features extracted from the latent layer of a pre-trained CNN in the nodes of a topological map that can be used to flexibly classify semantic properties of the mapped regions or to perform other types of visual tasks.

III. THE METHOD

The topological semantic mapping method presented in this work is inspired by SOM with time-varying structure [20] and uses the GoogLeNet, pre-trained on ImageNet [21] and available on the PyTorch library [22], to extract deep visual features from 2D images. An overview of the method is illustrated in Fig. 1 and Alg. 1 summarizes the topological

mapping and features consolidation processes. The following sections describe in detail the operation of the method.

A. Topology

At each time step k , the method receives as input a 2D image \mathbf{z}^k and its spatial position of capture $\mathbf{s}^k = \{s_i^k, i = 1 \dots n\}$ in the environment, where $n = 2$ in this work, but it could easily be extended to 3 dimensions for 3D maps. Each image is provided as input to the GoogLeNet, the output of the adaptive average pool 2D layer (which is the input of the linear classification layer in GoogLeNet) is flattened in the vector \mathbf{v}^k of $m = 1024$ dimensions and used as a visual features vector.

The topological map starts empty and is built as a graph. Each node j in the graph contains three vectors: $\mathbf{p}_j = \{p_{j1}, p_{j2}\}$, the spatial position of the node; $\mathbf{c}_j = \{c_{ji}, i = 1 \dots m\}$, the consolidated visual features vector; and $\boldsymbol{\delta}_j = \{\delta_{ji}, i = 1 \dots m\}$, the average features distance vector.

As the input data (\mathbf{v}^k and \mathbf{s}^k) is provided, the nodes compete to determine the topological location of the agent on the map and establish the nodes that will consolidate the visual features \mathbf{v}^k . The competition is performed using the spatial location provided, \mathbf{s}^k , and the winner is the node with the smallest spatial distance $D_e(\mathbf{s}^k, \mathbf{p}_j)$ to \mathbf{s}^k :

$$h(\mathbf{s}^k) = \arg \min_j [D_e(\mathbf{s}^k, \mathbf{p}_j)], \quad (1)$$

where $D_e(\mathbf{s}^k, \mathbf{p}_j)$ is calculated as the Euclidean distance between the given spatial position \mathbf{s}^k and the spatial position of the node \mathbf{p}_j :

$$D_e(\mathbf{s}^k, \mathbf{p}_j) = \sqrt{\sum_{i=1}^n (s_i^k - p_{ji})^2}. \quad (2)$$

If the map is empty or the spatial distance of the winning node to \mathbf{s}^k is not equal to or smaller than the spatial distance threshold λ , a new node η is inserted into the map with $\mathbf{p}_\eta = \mathbf{s}^k$, $\boldsymbol{\delta}_\eta = \mathbf{0}$, and the consolidated visual features vector \mathbf{c}_η initialized through an average between the input visual features \mathbf{v}^k and the current state of the consolidated visual features vector \mathbf{c}_l of the last visited node l , if any:

$$\mathbf{c}_\eta = \begin{cases} \gamma \mathbf{c}_l + (1 - \gamma) \mathbf{v}^k, & \text{if there is a } \mathbf{c}_l \\ \mathbf{v}^k, & \text{otherwise,} \end{cases} \quad (3)$$

where γ is the persistence rate, which determines how much of the consolidated visual features vector of the last visited node will persist on the new node.

If the spatial distance of the winning node is equal to or smaller than the spatial distance threshold λ , the node consolidates the input visual features \mathbf{v}^k as described in the next section (Section III-B). Moreover, whether there are other nodes with spatial distance higher, but equal to or smaller than λ , these nodes also consolidate the input visual features \mathbf{v}^k . This is because an image may be captured by the agent at an intersection position between nodes.

A connection between nodes is created whenever a transition occurs between them as the agent moves through the

environment, a transition is determined when the consecutive winning nodes are different. In addition, when a new node is inserted into the map, a connection is created between the new node and the previous winner, if any.

B. Visual Features Consolidation

The visual features in the input data are consolidated in the node j by updating the vector \mathbf{c}_j considering the learning rate $e \in]0, 1[$ and the Squared Euclidean distance, $D(\mathbf{v}^k, \mathbf{u}_j)$, between the visual features input vector \mathbf{v}^k and the last visual features vector consolidated in node j , \mathbf{u}_j :

$$\mathbf{c}_j(k+1) = \begin{cases} \mathbf{c}_j(k) + e(\mathbf{v}^k - \mathbf{c}_j(k)), & \text{if } D(\mathbf{v}^k, \mathbf{u}_j) \geq \tau \\ \mathbf{c}_j(k), & \text{otherwise,} \end{cases} \quad (4)$$

where τ is the minimum distance between the input features vector and the last features vector consolidated in the node, which prevents the node from consolidating very similar visual features vectors in sequence and, therefore, controls the visual habituation of the node. $D(\mathbf{v}^k, \mathbf{u}_j)$ is the Squared Euclidean distance described as follows:

$$D(\mathbf{v}^k, \mathbf{u}_j) = \sum_{i=1}^m (v_i^k - u_{ji})^2. \quad (5)$$

Moreover, the average features distance vector $\boldsymbol{\delta}_j$ of node j is updated through a moving average of the distance between the input visual features vector \mathbf{v}^k and the consolidated visual features vector \mathbf{c}_j based on the one introduced on [18]:

$$\boldsymbol{\delta}_j(k+1) = \begin{cases} (1 - e\beta)\boldsymbol{\delta}_j(k) + e\beta\boldsymbol{\phi}, & \text{if } D(\mathbf{v}^k, \mathbf{u}_j) \geq \tau \\ \boldsymbol{\delta}_j(k), & \text{otherwise,} \end{cases} \quad (6)$$

where $\beta \in]0, 1[$ controls the rate of change of the moving average, e is the learning rate, $\boldsymbol{\phi} = |\mathbf{v}^k - \mathbf{c}_j(k)|$ denotes the absolute value of each component of the resulting difference vector, and τ controls the visual habituation of the node. After the update, if \mathbf{c}_j and $\boldsymbol{\delta}_j$ were updated in relation to \mathbf{v}^k , then $\mathbf{u}_j = \mathbf{v}^k$.

C. Object and Place Classification

The current state of the consolidated visual features vector \mathbf{c}_j and the average features distance vector $\boldsymbol{\delta}_j$ of each node j , as well as the spatial position \mathbf{p}_j , can be used to obtain different types of semantic information about the mapped environment, as the objects present in regions, the categories of the mapped places or even to perform semantic topological localization.

In this work, the visual features consolidated in the vector \mathbf{c}_j are used to classify the objects visualized by the agent in the regions covered by each node j . For that, the vector \mathbf{c}_j of each node is provided to the linear classification layer of GoogLeNet and the classification outputs are obtained without the need of retraining. No softmax layer is used in the GoogLeNet in this work, so the final layer is the linear classification layer.

In addition, the visual features consolidated in the vector \mathbf{c}_j are also used to obtain the place categories of the regions

Algorithm 1: Topological Mapping and Features Consolidation

```

1 input: 2D image  $\mathbf{z}^k$  and spatial position  $\mathbf{s}^k$ 
2 output: The updated map and current node  $l$ 
3 function  $\text{map}(\mathbf{z}^k \text{ and } \mathbf{s}^k)$ :
4   Present the image  $\mathbf{z}^k$  to the GoogLeNet
5   Get the output of the adaptive average pool 2D layer
     as the visual features vector  $\mathbf{v}^k$ 
6   if  $\text{map}$  is empty then
7     Create new node  $\eta$  and set:  $\mathbf{p}_\eta \leftarrow \mathbf{s}^k$ ,  $\boldsymbol{\delta}_\eta \leftarrow \mathbf{0}$  and
        $\mathbf{c}_\eta$  as per Eq. 3
8     Set  $\mathbf{u}_\eta \leftarrow \mathbf{v}^k$ 
9     Assign  $l \leftarrow \eta$ , as the last winning node
10  else
11    Compute the spatial distance of all nodes to the
        position  $\mathbf{s}^k$  (Eq. 2)
12    Find the winner node  $h$  with the smallest spatial
        distance ( $d_h$ ) (Eq. 1)
13    if  $d_h > \lambda$  then
14      Create new node  $\eta$  and set:  $\mathbf{p}_\eta \leftarrow \mathbf{s}^k$ ,  $\boldsymbol{\delta}_\eta \leftarrow \mathbf{0}$ 
        and  $\mathbf{c}_\eta$  as per Eq. 3
15      Set  $\mathbf{u}_\eta \leftarrow \mathbf{v}^k$ 
16      Connect  $\eta$  to  $l$ 
17      Assign  $l \leftarrow \eta$ , as the last winning node
18    else
19      Update the vector  $\boldsymbol{\delta}_h$  of the winner and the
        other acceptable nodes with spatial distance
         $d \leq \lambda$ , if any (Eq. 6)
20      Update the vector  $\mathbf{c}_h$  of the winner and the
        other acceptable nodes with spatial distance
         $d \leq \lambda$ , if any (Eq. 4)
21      if  $h \neq l$  then
22        | Connect  $h$  to  $l$ 
23        Assign  $l \leftarrow h$ , as the last winning node
24    end
25  end

```

covered by each node j . A simple MLP implemented with the PyTorch library classifies the vector \mathbf{c}_j of each node and the place category is obtained. The MLP contains one hidden layer with 20 units and ReLU (Rectified Linear Unit) activation functions. Furthermore, the loss function used for training in the MLP was cross entropy and the optimizer was Adam [23]. In the experiments described in Section IV, the MLP is trained with visual features vectors of 1024 dimensions extracted from 2D images using the GoogLeNet, where the output of the adaptive average pool 2D layer is the visual features vector of each image used for training.

The classification of the objects visualized in each node and the place category of each node can be performed whenever necessary with the current state of the vector \mathbf{c}_j . The same could be done to classify other semantic properties of nodes if the CNN used has been trained for this type of classes or using a new classifier. The next section describes the use of the visual features data consolidated in the nodes to perform topological localization of 2D images.

D. Image Localization

To present the use of a generated map in other type of visual task, we use the consolidated visual features vector

\mathbf{c}_j and the average features distance vector $\boldsymbol{\delta}_j$ of each node j to localize 2D images on the map. The images have their features extracted using GoogLeNet, where the output of the adaptive average pool 2D layer is used as the visual features vector \mathbf{x} of each image. The node with the highest activation $ac(D_\omega(\mathbf{x}, \mathbf{c}_j), \boldsymbol{\omega}_j)$ represents the estimated location of the image on the map:

$$loc(\mathbf{x}) = \arg \max_j [ac(D_\omega(\mathbf{x}, \mathbf{c}_j), \boldsymbol{\omega}_j)]. \quad (7)$$

Thus, $\boldsymbol{\omega}_j$ is the relevance vector of the node j , in which each component is computed by an inverse logistic function based on the one proposed on [18]:

$$\omega_{ji} = \begin{cases} \frac{1}{1 + \exp\left(\frac{\delta_{ji} - \delta_{jimean}}{s(\delta_{jimax} - \delta_{jimin})}\right)}, & \text{if } \delta_{jimin} \neq \delta_{jimax} \\ 1, & \text{otherwise,} \end{cases} \quad (8)$$

where δ_{jimin} , δ_{jimax} and δ_{jimean} are respectively the minimum value, the maximum value and the average of the components of the distance vector $\boldsymbol{\delta}_j$. The parameter $s > 0$ controls the slope of the sigmoid function.

The activation $ac(D_\omega(\mathbf{x}, \mathbf{c}_j), \boldsymbol{\omega}_j)$ for each node j is calculated by a function of the weighted distance and the sum of the components of the relevance vector (introduced on [24]):

$$ac(D_\omega(\mathbf{x}, \mathbf{c}_j), \boldsymbol{\omega}_j) = \frac{\|\boldsymbol{\omega}_j\|_1}{D_\omega(\mathbf{x}, \mathbf{c}_j) + \|\boldsymbol{\omega}_j\|_1 + \varepsilon}, \quad (9)$$

where ε is a small value to avoid division by zero, $\|\cdot\|_1$ is the L^1 -norm, and $D_\omega(\mathbf{x}, \mathbf{c}_j)$ is the weighted Euclidean distance between the consolidated visual features vector and the image visual features vector, with weights given by the relevance vector:

$$D_\omega(\mathbf{x}, \mathbf{c}_j) = \sqrt{\sum_{i=1}^m \omega_{ji} (x_i - c_{ji})^2}. \quad (10)$$

Such an adaptive distance is validated in [18] and provides better results with high dimensional data.

IV. EXPERIMENTS

In this section, we detail the experiments performed to evaluate the topological semantic maps produced with the proposed method. The quality of the consolidated representations are evaluated in the tasks of object and place category recognition and image localization.

A. Dataset

We used in the experiments the COLD dataset, a real-world indoor dataset that has three indoor sub-datasets acquired in three different laboratories, COLD-Freiburg, COLD-Ljubljana, and COLD-Saarbrucken. Each sub-dataset contains data sequences acquired in different paths on the facilities. Not all data in the dataset was used due to inaccuracies in the position data in some data sequences. We selected for use in experimentation 18 data sequences of 6 paths, 3 sequences of each path. Of the total, 6 data sequences of

2 paths are from COLD-Freiburg, where path 1 is a sub-part of path 2. In addition, 12 sequences of 4 paths are from COLD-Saarbrucken, in which paths 1 and 3 are, respectively, sub-parts of paths 2 and 4. The sub-datasets have different types of data, but only 2D images from regular camera and their acquisition positions were used. The positions in the data were computed by the dataset authors with a laser-based localization technique. In all selected data, there are 11 place categories, 12592 images in COLD-Freiburg and 17700 in COLD-Saarbrucken.

B. Parameter Adjustment

The adjustment of almost all parameters of the proposed method for the following experiments was done using a parameter sampling technique, the Latin Hypercube Sampling (LHS) [25]. The spatial distance threshold λ was set manually since it directly affects the topology of the maps and the value 0.9 was used for all experiments. The parameter s of the image localization approach was also adjusted using the LHS. The LHS samples the parameters within previously established ranges and the ranges of each parameter are divided in subintervals of equal probability. Then, a single value is randomly chosen from each subinterval. Tab. I presents the ranges used for each parameter.

TABLE I
PARAMETER RANGES.

Parameters	min	max
Features learning rate (e)	0.001	0.1
Minimum distance (τ)	1.0	100.0
Persistence rate (γ)	0	1.0
Moving average rate (β)	0.001	1.0
Relevance smoothness (s)	0.001	0.1

C. Topology

In the proposed method, an adequate positioning of the nodes of the topological maps is vital for an adequate consolidation of the visual features. Thus, we evaluated the positioning of the nodes by checking if they were coherent with the spatial positions provided in the input data. For this, the data sequences that were captured in the same area were presented randomly to the method and a single map was generated per area, where each map was generated with 6 data sequences of 2 paths. The selected data contains a single area (paths 1 and 2) in COLD-Freiburg, and in COLD-Saarbrucken it contains area 1 (paths 1 and 2) and area 2 (paths 3 and 4).

The process was repeated 10 times per area and in each execution the positions of the nodes in the generated map were visually evaluated by plotting them over the positions of all input data. The results obtained allowed us to conclude that the nodes were positioned properly in all executions for all areas. We also analyzed all connections between the nodes and concluded that they all represented viable transitions in the environments. Fig. 2 shows a typical example.

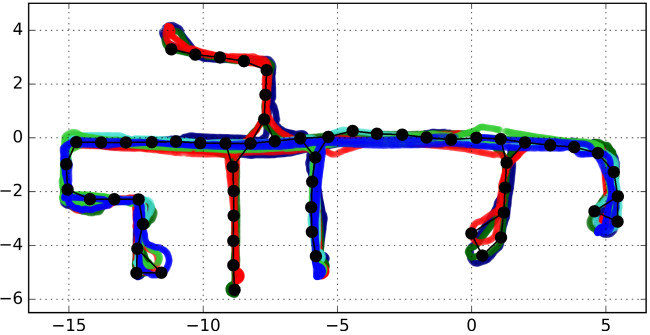


Fig. 2. Nodes of a topological map generated with the selected data sequences from the COLD-Freiburg dataset, provided to the proposed method in random order, plot over the positions of all the input data. Each colored line (there are six colors) represents the positions provided in a data sequence. The nodes of the map and their connections are in black.

D. Object Classification

In this evaluation, the consolidated visual features vector \mathbf{c}_j of each node j in the maps created is provided to the linear classification layer of the GoogLeNet and the classification output \mathbf{o}_j is obtained (as described in Section III-C). In addition, each image in the selected dataset is classified by GoogLeNet and the outputs for all the images captured around each node j of the maps are averaged in the vector \mathbf{m}_j . Here, as in the proposed method, images can be associated with more than one node as long as they have been captured in an intersecting position between nodes.

The classification output \mathbf{o}_j is compared to the mean output \mathbf{m}_j for each node j . All outputs are vectors with size b determined by the number of object classes selected and the comparison between them is made using the error function below, where $|\cdot|$ denotes the absolute value:

$$err_j = \frac{\sum_{i=1}^b |m_{ji} - o_{ji}|}{b}. \quad (11)$$

Then, the mean error for k nodes is calculated as follows:

$$err_{mean} = \frac{1}{k} \sum_{j=1}^k err_j. \quad (12)$$

This evaluation was done per sub-dataset, so for each sub-dataset, we have one experiment with all selected data sequences from all paths, with one map generated per data sequence. Thus, err_{mean} is calculated to evaluate all the nodes from all the generated maps as a single mean value for each dataset and so k in Eq. 12 assumes the number of nodes in all maps generated added.

We selected 13 classes of objects present on the ImageNet for this experiment, based on what is present on the images in COLD, they are: washbasin, soap dispenser, toilet seat, photocopier, monitor, desktop computer, desk, dining table, barber chair, microwave oven, stove, dishwasher and toaster. Therefore, b in Eq. 11 takes the value 13. Moreover, the average GoogLeNet output classification of all classes of objects for all images was 1.78 ± 1.51 for COLD-Freiburg and 2.34 ± 1.56 for COLD-Saarbrucken.

The first row of Tab. II presents the results, which suggest that the mapping model is capable of consolidating the visual features of regions in order to approximate the classification results to those of the average classification of all images captured in these regions, using the same CNN and classification layer without the need for retraining. They are especially good with the COLD-Freiburg data, where the results are lower than those obtained with the COLD-Saarbrucken. Notice that both errors measured are one order of magnitude smaller than the STD of the data.

However, in the results with the COLD-Saarbrucken, the errors observed in nodes located in bathrooms (0.322 ± 0.217) were worse than in the others. This has led to the variations observed in the results with this dataset. In particular, the standard deviation of 0.116. This may be related to some particular characteristic of these images when processed by GoogLeNet. We will investigate this issue in future work.

Tab. II also contains results with the proposed method without using the visual persistence capability (PM_{-VP}), which are not as good as those obtained with the complete proposed method (PM). This gives evidence of the positive contribution of the visual features persistence in the features consolidation.

TABLE II

RESULTS OF THE OBJECTS CLASSIFICATION EVALUATION. STANDARD DEVIATIONS ARE IN PARENTHESES.

errmean	COLD-Freiburg	COLD-Saarbrucken
PM^*	0.126(0.069)	0.189(0.116)
PM_{-VP}	0.172(0.106)	0.251(0.163)

* PM is Proposed Method and PM_{-VP} is Proposed Method without Visual Persistence.

E. Image Localization Experiment

In this experiment, we use the visual data consolidated in each node to localize images on the maps using the approach described in Section III-D. The experiment is performed using an adaptation of the k-fold cross-validation method. In which, each fold is a sequence of data selected from the datasets, k is the number of sequences chosen, and the order of the sequences is randomly selected. Thus, k-1 sequences of data are used in the generation of the map and all images in the remaining sequence of data are localized on the map. Therefore, in the experiment we use together only sequences of data that were captured in the same area and a single map is generated per area.

Tab. III shows the TOP 1 and TOP 5 accuracy values measured. TOP 1 evaluates whether for each image the node on the map with the highest activation is the node (or one of the nodes) in the ground truth. TOP 5 evaluates whether, for each image, one of the five nodes on the map with the highest activation is the node (or one of the nodes) in the ground truth. The ground truth for an image can be more than one node, as long as the image has been captured at an intersecting position between nodes.

The obtained results are promising and suggest that the consolidated representations in each node of the generated maps can be used to locate images captured around it. The localization results also provide evidence that the proposed method does not degrade its representations as more visual features are consolidated on the maps, since the TOP 1 and TOP 5 results obtained in conditions where the maps were created using all selected data per area (Fr1 - Fr2, Sa1 - Sa2 and Sa3 - Sa4 in Tab. III) were in the range of expected values, that is, higher than the ones using only the data from the larger paths per area (Fr2, Sa2, and Sa4 in Tab. III) and mostly smaller (in one case was higher) than the ones using only the data from the smaller paths (Fr1, Sa1, and Sa3 in Tab. III). Smaller paths tend to give better results since the number of nodes created in the maps are smaller.

Moreover, the results using only the data from path 1 (Fr1 in Tab. III) of the COLD-Freiburg were higher than the ones using only the data from path 2 (Fr2 in Tab. III), but smaller than expected. Path 1 (Fr1) is a subpart of path 2 (Fr2), therefore smaller and with similar visual characteristics. Therefore, it was expected higher results as the ones obtained with the data of COLD-Saarbrucken. The reason probably is related with the different illumination conditions in the images of the selected data from path 1 of COLD-Freiburg. This scenario will be used for experimentation in future work using also other CNN models. Lastly, it is also important to notice that even with different illumination conditions the localization results still improved using all selected data from COLD-Freiburg (Fr1 - Fr2 in Tab. III).

TABLE III

RESULTS OF THE IMAGE LOCALIZATION EXPERIMENT. STANDARD DEVIATIONS ARE IN PARENTHESES.

Data Sequences	TOP 1	TOP 5
Fr1(Cl1,Nt1,Nt3) - Fr2(Cl1,Cl2,Cl3)*	0.744(0.067)	0.907(0.033)
Fr1(Cl1,Nt1,Nt3)	0.719(0.114)	0.905(0.029)
Fr2(Cl1,Cl2,Cl3)	0.694(0.073)	0.885(0.040)
Sa1(Cl1,Cl2,Cl3) - Sa2(Cl1,Cl2,Cl3)	0.697(0.060)	0.911(0.029)
Sa1(Cl1,Cl2,Cl3)	0.754(0.032)	0.961(0.011)
Sa2(Cl1,Cl2,Cl3)	0.679(0.070)	0.890(0.046)
Sa3(Cl1,Cl2,Cl3) - Sa4(Cl1,Cl2,Cl3)	0.834(0.021)	0.976(0.016)
Sa3(Cl1,Cl2,Cl3)	0.843(0.028)	0.989(0.004)
Sa4(Cl1,Cl2,Cl3)	0.812(0.029)	0.965(0.011)

* Fr(n) is Freiburg (n = path 1 or 2), Sa(n) is Saarbrucken (n = path 1, 2, 3 or 4), Cl(n) is cloudy sequence (n = sequence 1, 2 or 3) and Nt(n) is night sequence (n = sequence 1 or 3).

We also studied the effect of the visual habituation (VH) capability. We evaluated this in two scenarios in which 10% of the images in each sequence were replicated 20 times in the first scenario and 40 times in the second. The images to be replicated were randomly selected at the beginning of the map construction in each execution from the data sequences used to build the map. With this, we simulate moments when the robot stops moving and captures very similar images for a while. Without visual habituation, this could degrade the consolidated representations stored in the respective node

due to the sequential presentation of similar features. Tab. V shows the results with the proposed method with (PM) and without visual habituation capability (PM_{-VH}). The results with the complete proposed method (PM) were all higher, what shows the positive influence of the visual habituation capability in the consolidation of visual features. Also, we can notice that the results with 40 times image replication were worse in PM_{-VH} , what suggests that without the visual habituation capability it would increasingly degrade its consolidated features the longer the robot stays put.

F. Place Classification

In the last experiment, the consolidated visual features vector c_j of each node j is feed into the MLP described in Section III-C to classify the nodes in one of the 11 place categories present in the dataset. This experiment is also performed using an adaptation of the k-fold cross-validation method, in which each fold is a sequence of data selected from the datasets and k is the number of sequences chosen. Thus, all images in the $k-1$ sequences of data are used to train the MLP in batch mode, with all images per epoch. The number of epochs is determined experimentally and only one is defined for each cross validation run. The remaining data sequence is used in the generation of the map and the resulting consolidated visual features vector c_j of each node j is classified by the MLP. In this experiment, for each execution we use together all selected data sequences that were captured in the two paths of the same area.

Tab. IV presents the excellent results obtained (classification accuracy), which suggest that even a simple MLP can be used to recognize accurately the place categories of the nodes from the visual features consolidated on it. Fig. 3 illustrates an example of the place classification results obtained with the map generated from a data sequence of COLD-Freiburg, in which we can see that only two nodes were misclassified by the MLP. Both nodes are located close to the borders between different place categories in the ground truth, from where it is possible to see the other regions, what may have led to the errors. For instance, there is a printer at the entrance to the printer area that is visible and close to the node located in the corridor, leading to the misclassification of this node as belonging to the printer area.

V. CONCLUSIONS

This paper presented a topological semantic mapping method that consolidates visual features of regions extracted from 2D images acquired in multiple views into the topological nodes of the generated maps. The consolidated features allow flexible classification of semantic properties of the regions covered by the nodes of the maps and use in a range of visual tasks. The experiments presented very promising results in indoor environments, which indicate that the consolidated features can be used to classify the objects seen in regions, recognize the place categories of regions, and locate images.

The experiments also suggest that the model does not degrade its consolidated representations with more data,

TABLE IV

RESULTS OF THE PLACE CLASSIFICATION EXPERIMENT. STANDARD DEVIATIONS ARE IN PARENTHESES AND THE SYMBOL — MEANS NO RESULTS AVAILABLE FOR THE SPECIFIC PLACE CATEGORY.

Accuracy	Fr1 and Fr2*	Sa1 and Sa2	Sa3 and Sa4
Corridor	0.987(0.018)	0.984(0.016)	1.000(0.000)
Printer area	1.000(0.000)	1.000(0.000)	1.000(0.000)
Robotics lab	—	0.944(0.078)	—
Stairs area	0.944(0.124)	—	—
Bathroom	1.000(0.000)	1.000(0.000)	1.000(0.000)
Kitchen	1.000(0.000)	—	0.970(0.043)
Terminal room	—	0.968(0.022)	—
Conference room	—	1.000(0.000)	—
1-person office	1.000(0.000)	0.933(0.094)	1.000(0.000)
2-person office	0.907(0.099)	0.917(0.186)	—
Large office	1.000(0.000)	—	—
Overall	0.979(0.021)	0.982(0.013)	0.995(0.011)

* Fr(n) is Freiburg (n = path 1 or 2) and Sa(n) is Saarbrucken (n = path 1, 2, 3 or 4).

however, new evaluations need to be performed to solidify the evidence. Therefore, it is future work to perform experiments focused on obtaining results to confirm the consistency of the consolidated representations over time, including other types of semantic properties. Furthermore, to assess the generalization ability of the method, we should also evaluate it with classifiers trained on images that are not from the environment used to generate the map. This would further evaluate the applicability of the consolidated representations.

In addition, the experiments in future work will be performed using other datasets and evaluate the method with CNNs other than GoogLeNet. More recent CNNs should provide even better results.

REFERENCES

- [1] I. Kostavelis and A. Gasteratos, “Semantic mapping for mobile robotics tasks: A survey,” *Robotics and Autonomous Systems*, vol. 66, pp. 86 – 103, 2015.
- [2] A. Pronobis and P. Jensfelt, “Large-scale semantic mapping and reasoning with heterogeneous modalities,” in *International Conference on Robotics and Automation (ICRA)*. IEEE, 2012, pp. 3515–3522.
- [3] N. Sunderhauf, F. Dayoub, S. Mcmahon, B. Talbot, R. Schultz, P. Corke, G. Wyeth, B. Upcroft, and M. Milford, “Place categorization and semantic mapping on a mobile robot,” in *International Conference on Robotics and Automation (ICRA)*, May 2016, pp. 5729–5736.
- [4] J. McCormac, A. Handa, A. Davison, and S. Leutenegger, “Semanticfusion: Dense 3d semantic mapping with convolutional neural networks,” in *IEEE International Conference on Robotics and Automation (ICRA)*, 2017, pp. 4628–4635.
- [5] D. Maturana, S. Arora, and S. Scherer, “Looking forward: A semantic mapping system for scouting with micro-aerial vehicles,” in *IEEE/RSJ International Conference on Intelligent Robots and Systems (IROS)*, 2017, pp. 6691–6698.
- [6] N. Sunderhauf, T. T. Pham, Y. Latif, M. Milford, and I. Reid, “Meaningful maps with object-oriented semantic mapping,” in *IEEE/RSJ International Conference on Intelligent Robots and Systems (IROS)*, 2017, pp. 5079–5085.
- [7] L. Ma, J. Stückler, C. Kerl, and D. Cremers, “Multi-view deep learning for consistent semantic mapping with rgb-d cameras,” in *IEEE/RSJ International Conference on Intelligent Robots and Systems (IROS)*, 2017, pp. 598–605.

TABLE V

RESULTS OF THE IMAGE LOCALIZATION EXPERIMENT WITH RANDOM IMAGE REPLICATION. STANDARD DEVIATIONS ARE IN PARENTHESES AND IR IS N° OF IMAGE REPLICATIONS.

IR	Data Sequences	PM ¹		PM _{-VH}	
		TOP 1	TOP 5	TOP 1	TOP 5
20	Fr1(Cl1,Nt1,Nt3) - Fr2(Cl1,Cl2,Cl3) ²	0.746(0.07)	0.904(0.02)	0.686(0.08)	0.883(0.05)
	Sa1(Cl1,Cl2,Cl3) - Sa2(Cl1,Cl2,Cl3)	0.693(0.06)	0.918(0.04)	0.672(0.07)	0.893(0.04)
	Sa3(Cl1,Cl2,Cl3) - Sa4(Cl1,Cl2,Cl3)	0.846(0.02)	0.976(0.02)	0.790(0.04)	0.968(0.02)
40	Fr1(Cl1,Nt1,Nt3) - Fr2(Cl1,Cl2,Cl3)	0.759(0.06)	0.902(0.02)	0.638(0.07)	0.880(0.03)
	Sa1(Cl1,Cl2,Cl3) - Sa2(Cl1,Cl2,Cl3)	0.693(0.05)	0.913(0.03)	0.650(0.08)	0.882(0.04)
	Sa3(Cl1,Cl2,Cl3) - Sa4(Cl1,Cl2,Cl3)	0.833(0.04)	0.976(0.02)	0.753(0.06)	0.951(0.02)

¹ PM is Proposed Method and PM_{-VH} is Proposed Method without Visual Habituation.

² Fr(n) is Freiburg (n = path 1 or 2), Sa(n) is Saarbrücken (n = path 1, 2, 3 or 4), Cl(n) is cloudy sequence (n = sequence 1, 2 or 3) and Nt(n) is night sequence (n = sequence 1 or 3).

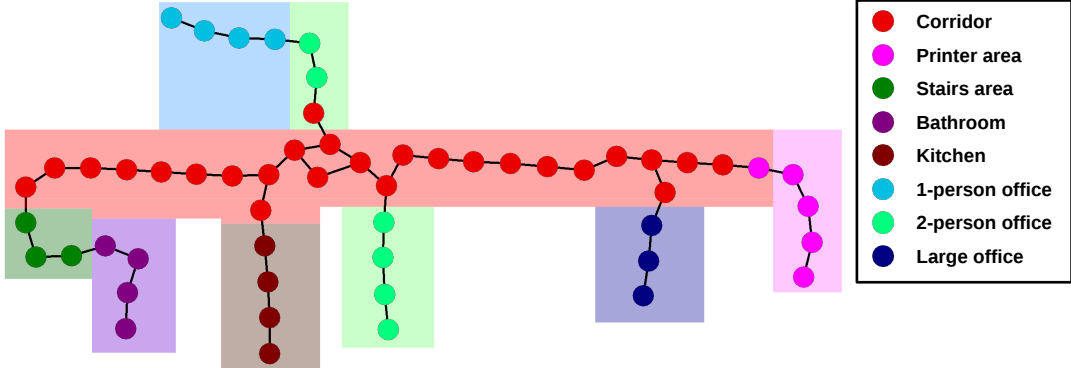


Fig. 3. Illustration of the place classification results obtained with the map generated from a data sequence of the path 2 in COLD-Freiburg. The color of each node is the class assigned by the MLP in the classification process and the colored blocks represent the place categories of the nodes covered by the blocks in the ground truth.

- [8] Y. Xiang and D. Fox, "Da-rnn: Semantic mapping with data associated recurrent neural networks," in *Robotics: Science and Systems*, Cambridge, Massachusetts, July 2017.
- [9] Y. C. N. Sousa and H. F. Bassani, "Incremental semantic mapping with unsupervised on-line learning," in *International Joint Conference on Neural Networks (IJCNN)*, July 2018.
- [10] D. Maturana, P.-W. Chou, M. Uenoyama, and S. Scherer, "Real-time semantic mapping for autonomous off-road navigation," in *Field and Service Robotics*, M. Hutter and R. Siegwart, Eds. Springer International Publishing, 2018, pp. 335–350.
- [11] F. Bernuy and J. Ruiz-del Solar, "Topological semantic mapping and localization in urban road scenarios," *Journal of Intelligent & Robotic Systems*, vol. 92, no. 1, pp. 19–32, 2018.
- [12] R. C. Luo and M. Chiou, "Hierarchical semantic mapping using convolutional neural networks for intelligent service robotics," *IEEE Access*, vol. 6, pp. 61 287–61 294, 2018.
- [13] Y. Nakajima and H. Saito, "Efficient object-oriented semantic mapping with object detector," *IEEE Access*, vol. 7, pp. 3206–3213, 2019.
- [14] J. C. Rangel, M. Cazorla, I. García-Varea, C. Romero-González, and J. Martínez-Gómez, "Automatic semantic maps generation from lexical annotations," *Autonomous Robots*, vol. 43, no. 3, pp. 697–712, 2019.
- [15] M. Grinvald, F. Furrer, T. Novkovic, J. J. Chung, C. Cadena, R. Siegwart, and J. Nieto, "Volumetric instance-aware semantic mapping and 3d object discovery," *IEEE Robotics and Automation Letters*, vol. 4, no. 3, pp. 3037–3044, 2019.
- [16] T. Roddick and R. Cipolla, "Predicting semantic map representations from images using pyramid occupancy networks," in *IEEE/CVF Conference on Computer Vision and Pattern Recognition (CVPR)*, June 2020.
- [17] C. Szegedy, W. Liu, Y. Jia, P. Sermanet, S. Reed, D. Anguelov, D. Erhan, V. Vanhoucke, and A. Rabinovich, "Going deeper with convolutions," in *IEEE Conference on Computer Vision and Pattern Recognition (CVPR)*, June 2015.
- [18] H. F. Bassani and A. F. R. Araujo, "Dimension selective self-organizing maps with time-varying structure for subspace and projected clustering," *IEEE Transactions on Neural Networks and Learning Systems*, vol. 26, no. 3, pp. 458–471, 2015.
- [19] A. Pronobis and B. Caputo, "Cold: The cosy localization database," *The International Journal of Robotics Research*, vol. 28, no. 5, pp. 588–594, 2009.
- [20] A. F. Araujo and R. L. Rego, "Self-organizing maps with a time-varying structure," *ACM Comput. Surv.*, vol. 46, no. 1, pp. 7:1–7:38, July 2013.
- [21] J. Deng, W. Dong, R. Socher, L.-J. Li, K. Li, and L. Fei-Fei, "ImageNet: A Large-Scale Hierarchical Image Database," 2009. [Online]. Available: <http://image-net.org/>
- [22] A. Paszke, S. Gross, F. Massa, A. Lerer, J. Bradbury, G. Chanan, T. Killeen, Z. Lin, N. Gimelshein, L. Antiga, A. Desmaison, A. Kopf, E. Yang, Z. DeVito, M. Raison, A. Tejani, S. Chilamkurthy, B. Steiner, L. Fang, J. Bai, and S. Chintala, "Pytorch: An imperative style, high-performance deep learning library," in *Advances in Neural Information Processing Systems 32*, 2019, pp. 8024–8035.
- [23] D. P. Kingma and J. Ba, "Adam: A method for stochastic optimization," *arXiv preprint arXiv:1412.6980*, 2014.
- [24] H. F. Bassani and A. F. R. Araujo, "Dimension selective self-organizing maps for clustering high dimensional," in *International Joint Conference on Neural Networks (IJCNN)*. IEEE, June 2012.
- [25] J. C. Helton, F. J. Davis, and J. D. Johnson, "A comparison of uncertainty and sensitivity analysis results obtained with random and latin hypercube sampling," *Reliability Engineering and System Safety*, vol. 89, pp. 305–330, 2005.